Miniaturized Hairpin Resonator Filters and Their Application to Receiver Front-End MIC's

MORIKAZU SAGAWA, KENICHI TAKAHASHI, AND MITSUO MAKIMOTO, MEMBER, IEEE

Abstract —**This paper describes the fundamental characteristics of newly developed miniaturized hairpin resonators having parallel coupled lines and shows their applications to bandpass filters and receiver front-end MIC's. A method for calculating filter coupling parameters using a general-purpose microwave circuit simulator is also presented.**

The bandpass filters using newly developed hairpin resonators have a suitable structure for microwave integrated circuits (MIC's), and the size of the experimental bandpass filters has been reduced to one half that of conventional hairpin resonators without increasing insertion losses.

Trial receiver front-end MIC's using these filters have also been developed and have shown good characteristics, for example, low noise and a high image suppression ratio. They are considered to be applicable to a higher frequency range above the *L*-band.

I. Introduction

THE INCREASING demand for mobile radio communication has caused a lack of frequency resources lower than 1 GHz. The time to fully utilize the *L*-band is now ripe. This technological trend requires the development of compact, low-loss resonators as fundamental elements of circuits in the *L*-band.

Microstrip half-wavelength open-ring resonators [1], [2], have attractive features above the *X*-band, and hairpin-shaped half-wavelength resonators [3] have been put to practical use, because their structure is adequate for compact bandpass filters. However, the size of these resonators is too large to design a filter in the *L*-band.

To make these resonators smaller in the UHF band, the authors previously proposed microstrip line split-ring resonators (MSR's) [4], [6], which are composed of a transmission line and a lumped element capacitor, suitable for MIC's. Dielectric split-ring resonators (DSR's) [5] were also developed to realize resonators that are more compact and have lower loss.

We have recently devised new hairpin-shaped split-ring resonators with parallel coupled lines to replace the lumped element capacitor. They can also be applied to a much higher frequency range than previously described MSR's and DSR's. The filters incorporating these resonators are less than half the size of those with conventional hairpin resonators. These filters have the advantage that frequency adjustment can be easily achieved by trimming the length of the parallel coupled lines.

Manuscript received March 30, 1989; revised July 17, 1989.

The authors are with the Tokyo Research Laboratory, Matsushita Electric Industrial Company, Ltd., Higashimita, Tama-ku, Kawasaki 214, Japan.

IEEE Log Number 8930949.

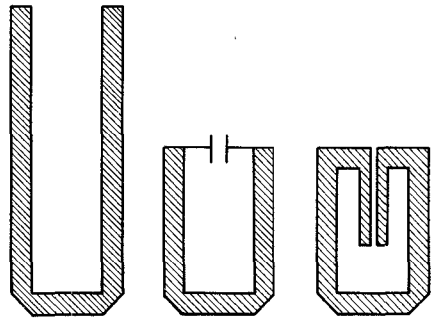

Fig. 1. Some structural variations of the hairpin resonator. (a) Conventional hairpin resonator. (b) Miniaturized hairpin resonator. (c) Miniaturized hairpin resonator having coupled lines.

This paper describes the resonance properties of newly developed compact hairpin-shaped split-ring resonators, a design method for bandpass filters using these resonators, and their application to receiver front-end MIC's in the *L*-band.

First, some structural variations of split-ring resonators are summarized and fundamental characteristics such as resonance properties are analytically derived. Second, a method for calculating filter coupling parameters using a general-purpose microwave circuit simulator is discussed, and three design charts which are required in designing bandpass filters are prepared. Third, to verify this filter synthesis method, an experimental bandpass filter is designed and fabricated. The experimental performance data are shown to be in close agreement with the design results. Finally, an experimental *L*-band mixer using a diplexer composed of these filters is constructed, and the results make it clear that it has good electrical performance as a receiver front end.

II. Resonance Properties

A. Resonator Structure

Some structures of microstrip line hairpin resonators are shown in Fig. 1. Fig. 1(a) shows a conventional hairpin resonator, but it is too large to realize bandpass filters below the *L*-band.

0018-9480/89/1200-1991$01.00 ©1989 IEEE

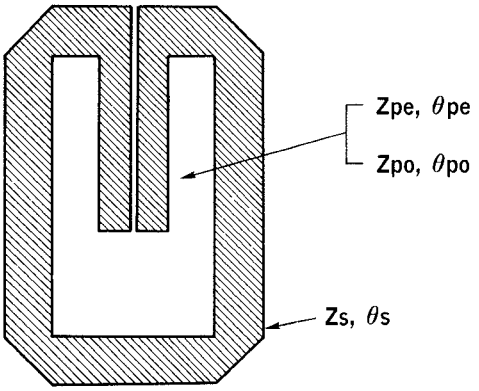

Fig. 2. Electrical parameters of the compact hairpin resonator.

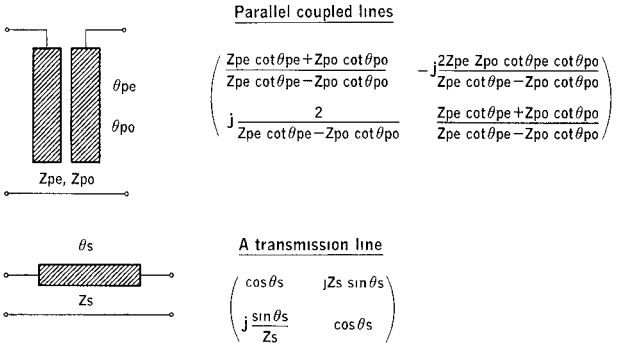

Fig. 3. Parallel coupled lines, a transmission line, and their *ABCD* matrices.

To reduce the size of conventional hairpin resonators, we previously introduced the split-ring resonator. It is composed of a transmission line and a capacitor which connects at both ends of the line. It should be noted that this resonator structure has no RF short-circuited points, which often generate parasitic components. Fig. 1(b) shows a hairpin-shaped split-ring resonator. It is desirable to choose a hairpin-shaped structure in designing compact multistage filters which have a parallel coupled section for interstage coupling.

Fig. 1(c) shows a newly developed hairpin-shaped split-ring resonator, which has an improved structure compared with the one in Fig. 1(b); parallel coupled lines with an open-circuited end have been adopted in place of the lumped element capacitor. This structure can also be applied to a much higher frequency range than that mentioned above using the lumped element capacitor, and this configuration is suitable for MIC's because it can be made using a photo etching process.

The advantages of this type of resonator include

1) small size, with no Q-value degradation,
2) expansion of the applicable frequency range,
3) easy adjustment of resonance frequency.

B. Resonance Conditions

The resonance conditions of split-ring resonators can be obtained using the *ABCD* matrices, which express a transmission line and a capacitor, respectively. The resonance condition of the structure shown in Fig. 1(b) is the same as that of the previously proposed split-ring resonator with a lumped element capacitor [4], [6]. The resonator shown in Fig. 1(c) is considered here. It can be analyzed using the following parameters, as also shown in Fig. 2.

Z_s	characteristic impedance of the single line,
θ_s	electrical length of the single line,
Z_{pe}, Z_{po}	even- and odd-mode impedance of the parallel coupled lines,
θ_{pe}, θ_{po}	even- and odd-mode electrical length of the parallel coupled lines.

Using these parameters, the *ABCD* matrix for parallel coupled lines with an open end [7] and a transmission line can be expressed as shown in Fig. 3.

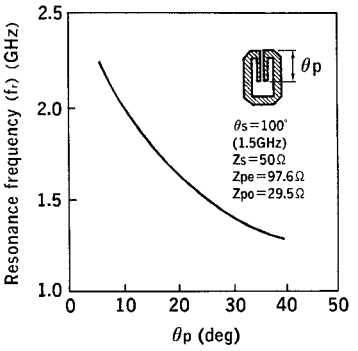

Fig. 4. Calculated results of a resonance frequency.

The resonance condition can be calculated from the input admittance using the total *ABCD* matrix. The results are as follows:

$$\left(Z_{pe}Z_{po}\cot\theta_{pe}\cot\theta_{po}-Z_s^2\right)\sin\theta_s + Z_s\left(Z_{pe}\cot\theta_{pe}+Z_{po}\cot\theta_{po}\right)\cos\theta_s - Z_s\left(Z_{pe}\cot\theta_{pe}-Z_{po}\cot\theta_{po}\right)=0. \quad (1a)$$

When $\theta_{pe}=\theta_{po}=\theta_p$, (1a) is simplified to

$$\left(Z_{pe}Z_{po}\cot\theta_p-Z_s^2\tan\theta_p\right)\sin\theta_s + Z_s\left(Z_{pe}+Z_{po}\right)\cos\theta_s - Z_s\left(Z_{pe}-Z_{po}\right)=0. \quad (1b)$$

Even- and odd-mode phase velocities are dependent upon properties of the substrate and line structure. Therefore, we introduced (1b) to analyze the resonance characteristics in the following discussion.

Fig. 4 shows one of the calculated relationships between the fundamental resonance frequency and the electrical length of the parallel coupled lines, where $Z_s=50\Omega$, $\theta_s=100°$, $Z_{pe}=97.6\Omega$, $Z_{po}=Z_s^2/Z_{pe}=29.5\Omega$.

These results clearly indicate that fine frequency tuning can be easily achieved by adjusting the length of the parallel coupled lines during the manufacturing process.

C. Equivalent Circuits at Resonance Points

The resonance conditions expressed above are general descriptions derived from the input admittance of the resonator. However, their relationship is too complicated

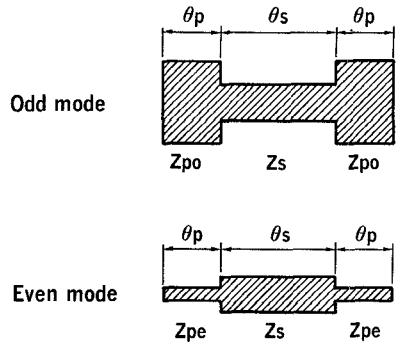

Fig. 5. Equivalent circuits at resonance points.

to allow an understanding of their physical meanings. Let us investigate the resonance conditions from the viewpoint of the equivalent circuit at resonance. Parallel coupled lines with an open-circuited end are considered to have either an odd-mode or an even-mode electromagnetic field distribution at resonance. Therefore, two equivalent circuits must exist, as shown in Fig. 5. These resonators are found to be stepped impedance resonators (SIR's) [8], and their resonance conditions are as follows:

$$\text{odd mode:} \quad \tan(\theta_s/2)\cdot\tan\theta_p = K_o = Z_{po}/Z_s \quad (2a)$$

$$\text{even mode:} \quad \tan(\theta_s/2)\cdot\tan\theta_p = K_e = Z_{pe}/Z_s. \quad (2b)$$

The fundamental resonance frequency occurs in the odd mode, and the next higher resonance frequency (the lowest spurious frequency) in the even mode. In this way, higher mode resonance frequencies alternate between odd and even.

The method discussed in the previous section is indispensable in a detailed analysis of the resonators. However, the equivalent circuits mentioned above are enough to facilitate analysis of the resonance frequencies of the fundamental and the higher mode. Then, the calculated results obtained by solving (2a) agree well with the results shown in Fig. 4.

III. Filter Design Parameters

A. Theoretical Background of Simulations

To design bandpass filters, it is necessary to obtain coupling parameters such as the external Q (Q_e) and the interstage coupling factor k. Let us consider a method for calculating the above-mentioned coupling parameters using generalized inverter and resonator circuits.

First, we discuss the theoretical background and a method for obtaining the unloaded Q (Q_0) and the external Q (Q_e) simultaneously. Fig. 6(a) shows an equivalent circuit of an input and output coupling circuit, where J_0 and $Y(\omega)$ represent the generalized admittance inverter parameter and the admittance for the resonator, respectively.

$$Y(\omega) = G_0 + jB(\omega) = G_0 + jb_0(\omega/\omega_0 - \omega_0/\omega) \quad (3)$$

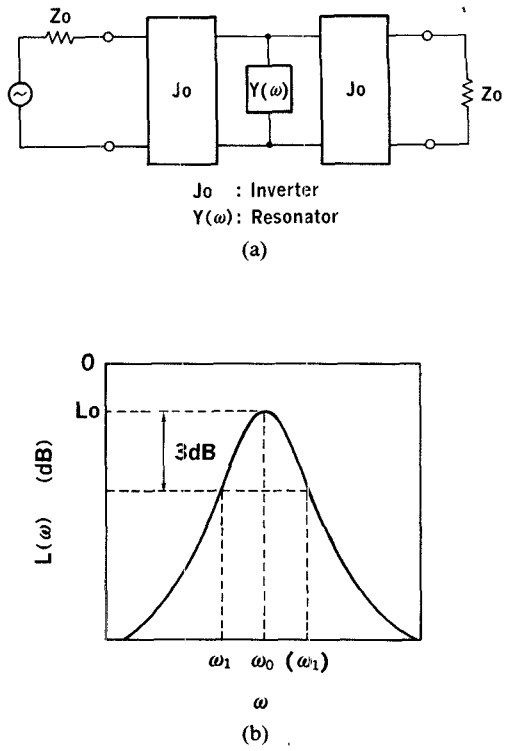

Fig. 6. An equivalent circuit and a frequency response of an input and output coupling circuit.

where

G_0 conductance of the resonator,
b_0 slope parameter of the resonator,
ω_0 resonance angular frequency.

The elements of the $ABCD$ matrix for Fig. 6(a) can be expressed as

$$A = D = -1$$
$$B = -G_0/J_0^2 - jb_0(\omega/\omega_0 - \omega_0/\omega)/J_0^2$$
$$C = 0. \quad (4)$$

Then, by calculating the insertion loss known as transducer loss (defined by the ratio of the power available from the source to the power absorbed by the load [9]), we can obtain

$$L(\omega) = \frac{1}{4}\left\{\left(2+\frac{Q_e}{Q_0}\right)^2 + Q_e^2(\omega/\omega_0 - \omega_0/\omega)^2\right\} \quad (5)$$

where

$$Qe = b_0/Z_0J_0^2 \qquad Q_0 = b_0/G_0.$$

The frequency response of (5) is shown in Fig. 6(b), where ω_1 is the angular frequency of 3 dB down points. The insertion losses at $\omega = \omega_0$ and $\omega = \omega_1$ represent $L(\omega_0)$ and $L(\omega_1)$ respectively:

$$L(\omega_0) = L_0 = 1 + \frac{Qe}{Q_0} + \frac{1}{4}\left(\frac{Qe}{Q_0}\right)^2 \quad (6)$$

$$L(\omega_1) = 2L_0 = 1 + \frac{Qe}{Q_0} + \frac{1}{4}\left(\frac{Qe}{Q_0}\right)^2 + \frac{1}{4}Qe^2\cdot\Omega_1^2 \quad (7)$$

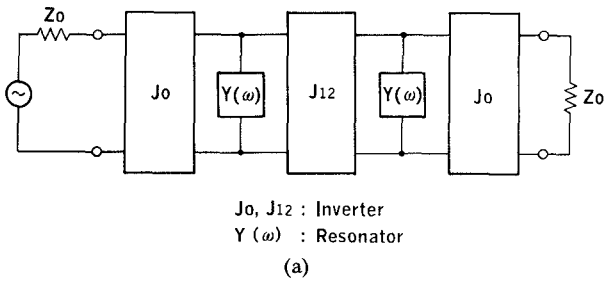

(a)

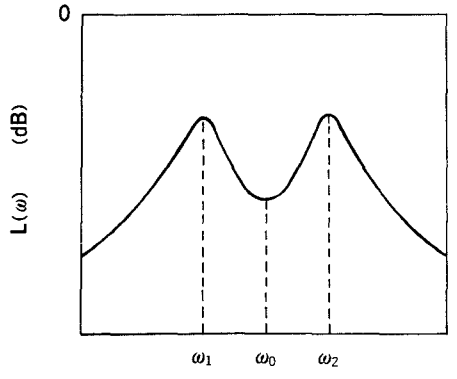

(b)

Fig. 7. An equivalent circuit and a frequency response of a resonator pair.

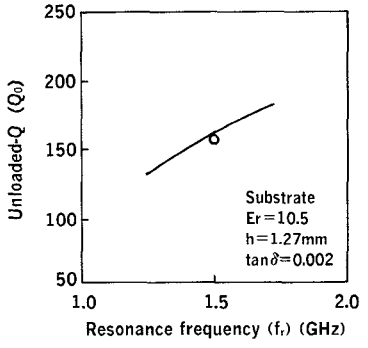

Fig. 8. Filter design parameters: unloaded Q (Q_0).

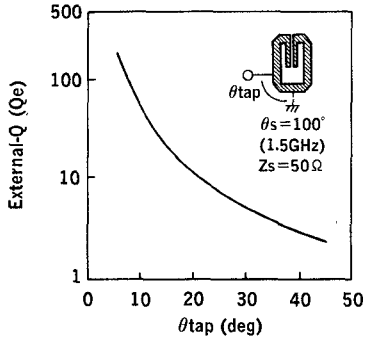

Fig. 9. Filter design parameters: external Q (Q_e).

where

$$\Omega_1 = |\omega_1/\omega_0 - \omega_0/\omega_1|.$$

From (6) and (7) the unloaded Q (Q_0) and the external Q (Q_e) are expressed as a function of the angular frequencies ω_0 and ω_1 and their insertion losses:

$$Qe = \frac{2}{\Omega_1}\sqrt{L_0} \qquad Q_0 = \frac{\sqrt{L_0}}{\Omega_1\left(\sqrt{L_0}-1\right)}. \tag{8}$$

Equation (8) indicates that the external Q (Q_e) and the unloaded Q (Q_0) can be calculated from the frequency responses obtained by a general-purpose microwave circuit simulator.

Next, we consider the interstage coupling factor k [6]. Fig. 7(a) illustrates a generalized equivalent circuit of a resonator pair. The interstage coupling factor k can be derived by procedures similar to those mentioned above. Insertion loss $L(\omega)$ is expressed as follows:

$$L(\omega) = \frac{B(\omega)^4 - 2\left\{J_{12}^2 - \left(G_0 + J_0^2 Z_0\right)^2\right\}B(\omega)^2 + \left\{J_{12}^2 + \left(G_0 + J_0^2 Z_0\right)^2\right\}^2}{4J_{12}^2 J_0^4 Z_0^2}. \tag{9}$$

There are two maximum values for $L(\omega)$ if $J_{12} > G_0 + J_0^2 Z_0$ as shown in Fig. 7(b). Let their angular frequencies be ω_1 and ω_2. Then we have the following equation:

$$\frac{\omega_2 - \omega_1}{\omega_0} = \frac{1}{b_0}\sqrt{J_{12}^2 - \left(G_0 + J_0^2 Z_0\right)^2}. \tag{10}$$

The relationship between the admittance slope parameter b_0 and the interstage coupling factor k is expressed by

$$J_{12} = b_0 \cdot k. \tag{11}$$

Then

$$k = \sqrt{\left(\frac{\omega_2 - \omega_1}{\omega_0}\right)^2 + \left(\frac{1}{Qe} + \frac{1}{Q_0}\right)^2}. \tag{12}$$

The circuit simulation can take large values for Q_e and Q_0 independently (for example about 10^4), which is different from the experimental method. Therefore, we have k as shown in (13) with an error less than 1 percent in the region of $k > 10^{-2}$:

$$k = \frac{\omega_2 - \omega_1}{\omega_0}. \tag{13}$$

Equations (12) and (13) also indicate that it is possible to calculate the interstage coupling factor k when the frequency response, as shown in Fig. 7(b), is obtained by a circuit simulation.

B. Filter Design Charts

The calculated results of coupling parameters indispensable in designing filters are shown in Figs. 8 to 10. These parameters can be calculated on the basis of the above discussion. In this example, the unloaded Q was calculated

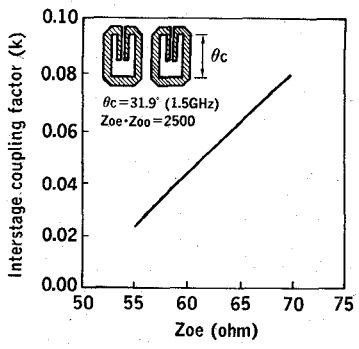

Fig. 10. Filter design parameters: interstage coupling factor k.

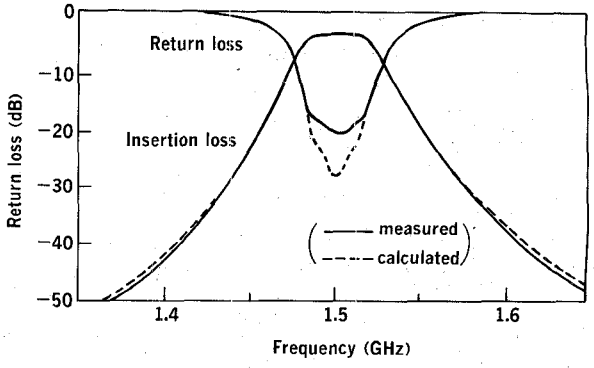

Fig. 12. Characteristics of the experimental filter.

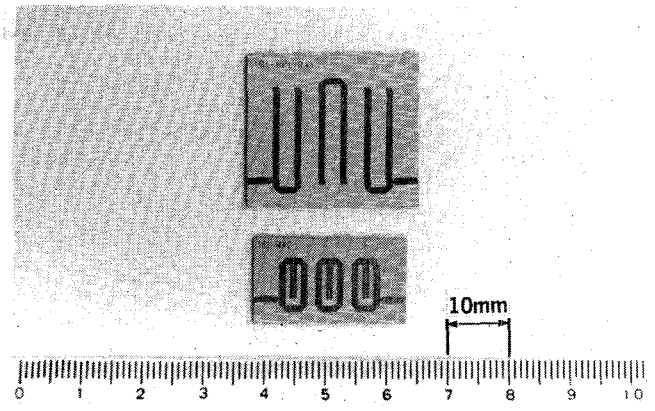

Fig. 11. Photograph of the experimental filter. Upper pattern: conventional hairpin resonator filter. Lower pattern: newly developed hairpin resonator filter.

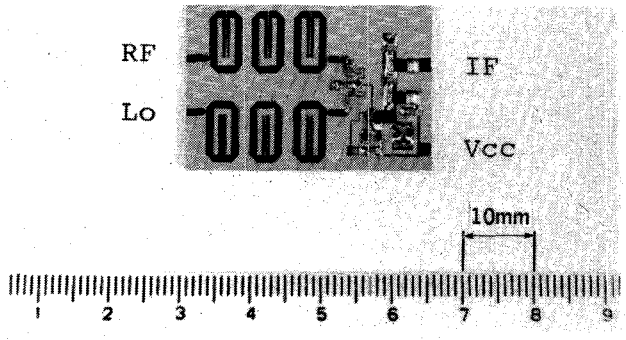

Fig. 13. A photograph of the experimental mixer.

where the substrate has a dielectric constant $E_r = 10.5$, a thickness $h = 1.27$ mm, a copper resistivity $\rho = 1.673\,\mu\Omega\cdot$cm and a loss tangent $\tan\delta = 0.002$, as shown in Fig. 8. The round dot in Fig. 8 indicates the measured results where $Q_0 = 155$, about 10 percent less than that of a conventional hairpin resonator. Input and output coupling, expressed as external Q (Q_e), is achieved by tapping where $\theta s = 100°$ (1.5 GHz) and $Z_s = 50\ \Omega$, as shown in Fig. 9; interstage coupling between resonators is achieved by parallel line coupling where $\theta_c = 31.9°$ (1.5 GHz) and $Z_{0e}\cdot Z_{0o} = 2500$, as shown in Fig. 10. In the process of calculating external Q (Q_e), the length of the parallel coupled lines (θ_p) were adjusted to keep the resonance frequency the same by using the optimization function of a simulator.

IV. Applications

On the basis of the above results, bandpass filters and receiver front-end MIC's were developed.

A. Bandpass Filters

Fig. 11 shows the MIC layouts of two experimental filters designed with the same electrical specifications, such as center frequency, bandwidth, and attenuation. One (the upper pattern) is a conventional hairpin resonator filter; the other (the lower pattern) is a newly developed miniaturized hairpin resonator filter. The lower filter has a size less than half that of the upper one.

The filter design parameters for the miniaturized hairpin-shaped split-ring resonator are as follows ($f = 1.5$ GHz):

resonator parameters:	$Z_s = 50\ \Omega$, $\theta_s = 100°$, $Z_{pe} = 97.6\ \Omega$, $Z_{po} = 29.5\ \Omega$, $\theta_p = 26°$
filter parameters:	tapping position: $\theta_{tap} = 13.8°$
	interstage coupling: $Z_{0e} = 57.2\ \Omega$, $Z_{0o} = 43.7\ \Omega$, $\theta_c = 31.9°$.

The filter was fabricated with a substrate similar to that indicated in Fig. 8. The spacing between the resonators for interstage coupling becomes narrow because the length of the parallel coupling lines is considerably less than 90°, which is typical of conventional hairpin resonator filters.

Fig. 12 shows the measured and the calculated response of the newly developed three-stage bandpass filter (BPF). These frequency responses agree well with the computer simulation results.

The unloaded $Q(Q_o)$ of the newly developed hairpin resonator is 10 percent less than that of a conventional one, as mentioned before; nevertheless the passband insertion loss is less than 3.5 dB, approximately the same as that for conventional hairpin BPF's. Thus, it can be concluded that miniaturization of the resonator slightly influences the passband insertion loss.

B. Receiver Front End

Fig. 13 shows the experimental transistor mixer, which uses a diplexer composed of receiver and local oscillator BPF's. This mixer was developed for receiver front ends in mobile communication equipment, which must be com-

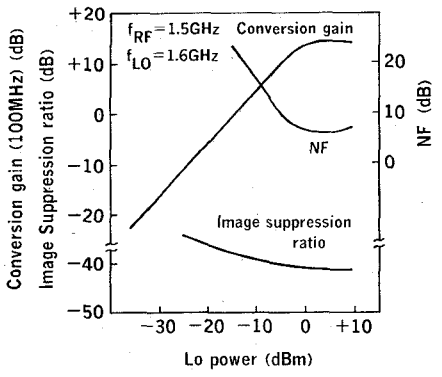

Fig. 14. Characteristics of the experimental mixer.

pact, inexpensive, and have low power consumption. This mixer utilizes a silicon bipolar transistor and is fabricated on a printed circuit board, the same as that of the experimental BPF.

Fig. 14 shows the measured data of this mixer. These data show that the conversion gain is 12.6 dB and NF is 7.4 dB when local oscillator power is 0 dBm. This mixer also has good image suppression characteristics (more than 41.5 dB) and low power consumption (12 mW). The net NF value of this mixer after subtracting the receiver BPF losses should be about 3.5 dB, which approximately corresponds to the amplifier NF value using the same transistor.

This mixer configuration is also applicable to the higher frequency range above the *L*-band.

V. Conclusions

A miniaturized hairpin-shaped split-ring resonator with parallel coupled lines was developed and its resonance properties were analytically derived.

A method for calculating coupling parameters using a general-purpose microwave simulator was demonstrated, and one set of design charts was prepared for designing a trial bandpass filter.

The experimental bandpass filter showed excellent performance, as seen in its compact size and low insertion losses, and its frequency responses indicated close coincidence with the design results. The trial receiver front end using these filters also showed good characteristics, among them low noise and high image suppression ratio. These results made it clear that both bandpass filters using newly developed compact split-ring resonators and receiver front ends incorporating them have many advantages for application to mobile radio equipment.

Acknowledgment

The authors gratefully acknowledge the assistance of many colleagues at the Tokyo Research Laboratory, Matsushita Electric Industrial Co., Ltd.

References

[1] F. C. de Ronde and S. Shammas, "MIC band filters using open-ring resonators," in *Proc. 4th European Microwave Conf.*, 1974, pp. 531–535.

[2] I. Wolff and V. K. Tripathi, "The microstrip open-ring resonator," *IEEE Trans. Microwave Theory Tech.*, vol. MTT-32, pp. 102–107, Jan. 1984.

[3] E. G. Cristal and S. Frankel, "Hairpin-line and hybrid hairpin-line/half-wave parallel-coupled-line filters," *IEEE Trans. Microwave Theory Tech.*, vol. MTT-20, pp. 719–728, Nov. 1972.

[4] M. Makimoto and M. Sagawa, "Varactor tuned bandpass filters using microstrip-line ring resonators," in *IEEE MTT-S Int. Microwave Symp. Dig.*, May 1986, pp. 411–414.

[5] M. Sagawa, I. Ishigaki, M. Makimoto, and T. Naruse, "Dielectric split-ring resonators and their application to filters and oscillators," in *IEEE MTT-S Int. Microwave Symp. Dig.*, May 1988, pp. 605–608.

[6] M. Makimoto "Microstrip-line split-ring resonators and their application to bandpass filters," *Trans. IEICE Japan*, vol. J71-C, no. 7, pp. 1063–1070, July 1988.

[7] G. I. Zysman and A. K, Johnson, "Coupled transmission line networks in an inhomogeneous dielectric medium," *IEEE Trans. Microwave Theory Tech.*, vol. MTT-17, pp. 753–759, Oct. 1969.

[8] M. Makimoto and S. Yamashita, "Bandpass filters using parallel coupled strip-line stepped impedance resonators," *IEEE Trans. Microwave Theory Tech.*, vol. MTT-28, pp. 1413–1417, Dec. 1980.

[9] G. Matthaei, L. Young, and E. M. T. Jones, *Microwave Filters, Impedance-Matching Networks, and Coupling Structures*. New York: McGraw-Hill, 1964.

Morikazu Sagawa was born in Tokyo, Japan, on May 13, 1949. He received the B.S. degree in electronic engineering from the University of Electro-Communications, Tokyo, Japan in 1973.

In 1973 he joined the Matsushita Research Institute Tokyo, Inc., Kawasaki, Japan. There he did research and development work on microwave components, in particular filters and oscillators. In 1987 he was transferred to Tokyo Research Laboratory of Matsushita Electric Industrial Co., Ltd., Kawasaki, Japan. He is presently concerned with RF analog integrated circuits and radio equipment for land mobile communication.

Mr. Sagawa is a member of the Institute of Electronics, Information and Communication Engineers (IEICE) of Japan.

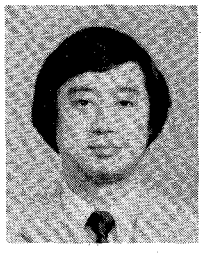

Kenichi Takahashi was born in Akita, Japan, on February 13, 1953. He received the B.S. degree in electronic engineering from the University of Electro-Communications, Tokyo, Japan, in 1975.

In 1975, he joined the Matsushita Research Institute Tokyo, Kawasaki, Japan. From 1975 to 1984, he worked on thermal image processing technology using pyroelectric sensors. Beginning in 1984, he did research and development work on CATV tuners. In 1987, he was transferred to the Tokyo Research Laboratory, Matsushita Electric Industrial Co., Ltd., where he is currently concerned with radio equipment for digital communication.

Mr. Takahashi is a member of the Institute of Television Engineers of Japan.

Mitsuo Makimoto (M'87) was born in Kagoshima, Japan, on September 19, 1944. He received the B.S. and M.S. degrees in electrical engineering from Yokohama National University, Yokohama, Japan, in 1968 and 1970, respectively.

In 1970, he joined the Matsushita Research Institute Tokyo, Kawasaki, Japan, where he did research and development work on microwave integrated circuits and components for radio communication systems. In 1987, he was transferred to Tokyo Research Laboratory, Matsushita Electric Industry Co., Ltd., Kawasaki, Japan, where he has been engaged in research on microwave devices and subsystems for advanced mobile communication systems.

Mr. Makimoto is a member of the Institute of Electronics, Information and Communication Engineers of Japan and the Institute of Television Engineers of Japan.